Investigating the Measurement Capability of Densely-Distributed Subdermal EEG Electrodes

Narayan Puthanmadam Subramaniyam*, Katrina Wendel*, Atte Joutsen, and Jari Hyttinen
Department of Biomedical Engineering
Tampere University of Technology
Tampere, Finland 33101
*Corresponding Authors: narayan.puthanmadamsubramaniyam@tut.fi & katrina.wendel@tut.fi

***Abstract*—This paper studies the effect of bipolar subdermal EEG lead placement on measurement sensitivity distributions. The electrodes were subdermally located on the skull of a realistic human head and arranged in a 5×5 matrix of electrodes located at the apex of the cranial vault. The effects on the measurement sensitivity were studied by means of the half-sensitivity volume (HSV). The results indicate that subdermal measurements focus the accuracy and specificity of EEG measurement; however, the size of the half sensitivity volume varies due to electrode location across one or more gyri, gray matter and cerebrospinal fluid (CSF) thickness. The results of the study suggest that subdermal needle electrodes could provide specific and accurate measurements of cortical activation but warrant further studies to understand how much the measurement sensitivity is influenced by placement of the subdermal electrodes over the gyri versus sulci.**

I. Introduction

Improving the measurement resolution of electroencephalography (EEG) electrodes requires reducing the electrode size and locating it subdermally. Traditional surface EEG electrodes measure electrical activity from a much larger area of the brain than subdermal needle electrodes [1], [2]. Ideally, subdermal electrodes should be inserted against the skull and insulated down to the tip. Subdermal needle electrodes are commonly used in clinical electromyography (EMG), which are inserted into the muscles of interest, but are less commonly used in EEG and evoked potential (EP) studies. These minimally-invasive measurement electrodes offer higher spatial resolution due to their concentrated lead field currents that are not diffused by the skin.

Over the last four decades researchers have experimentally tested the subdermal electrodes as a possible substitute for surface electrodes [3]–[8]. Many of the early studies claimed that the subdermal needle electrodes yielded similar waveform and latency data for EP trials with a sufficient number of epochs as surface cup electrodes [3]–[5]. Bispectral index (BIS) studies began comparing surface and subdermal electrode types for ease of use and practicality and similarly concluded that amplitudes and latencies correlated between electrode types [6], [9], [10]. However, [11], [12] advised that cortical activity should be evaluated on an individual basis rather than relying upon a sole number to indicate depth of anesthesia because BIS suffers from the EEG inverse problem of non-uniqueness [13]. It is clear that there is a need for subdermal electrodes in the intensive care or operating room, patients even prefer the needle electrodes [14], and they can be used for extended periods [8]. What these studies lack and what is often inquired about is a clear understanding of what the subdermal electrode really measures.

In the present study we apply the concept of the half-sensitivity volume (HSV) to analyze the effects of EEG electrode implantation on the measurement sensitivity distribution within the brain. Specifically, we aim to identify optimal high resolution measurement sensitivity distributions associated with implanted electrodes.

II. Methods

A. Sensitivity distribution

This study simulated the sensitivity distributions of twenty-four bipolar subdermal EEG leads. The lead field maps the direction and sensitivity of each measurement lead [15], [16]. It is created by feeding a reciprocal current I_R to the measurement lead. There are two ways to explain and depict the lead field – either as a current field or a potential field. In this study the results map the lead field currents. The lead voltage relates the measured signal to the current sources in the volume conductor such that

$$V_{LE} = \int_v \frac{1}{\sigma} \mathbf{J}_{LE} \cdot \mathbf{J}^i dv, \tag{1}$$

where V_{LE} is the measured EEG voltage in the volume conductor v. The reciprocal current field $\mathbf{J}_{LE}$ is the lead field, $\mathbf{J}^i[A/m^2]$ is the impressed current density field in the volume conductor, and σ is the conductivity tensor [S/m] [16].

The sensitivity distribution in the volume conductor can be established by applying the reciprocity theorem of Helmholtz with the Poisson equation (Eq. 2) applied to describe quasi-static bioelectric source-field problems [17], [18]. A source distribution, $\mathbf{J}^i$, containing only reciprocal source currents at the measurement electrodes raises a gradient potential distribution, $\nabla\Phi$, i.e. measurement sensitivity, according to the linear Poisson equation

$$\nabla \cdot (\sigma \nabla \Phi) = \nabla \cdot \mathbf{J}^i \,(\text{in } \Omega), \tag{2}$$

setting the Neumann boundary conditions equal to zero on the scalp

$$\sigma(\nabla \Phi) \cdot \mathbf{n} = 0 \,(\text{on } \Gamma_\Omega), \tag{3}$$

978-1-4244-8281-8/11/$26.00 ©2011 IEEE

TABLE I
TISSUES AND CONDUCTIVITY (RESISTIVITY) VALUES INCLUDED IN OUR REALISTIC HEAD MODEL [22].

Tissue	Conductivity [S/m]	Resistivity [Ω cm]
Bone marrow	0.046	2180
Fat	0.04	2500
Skull/Bones	0.029	3450
White matter	0.14	700
Gray matter	0.33	300
Scalp	0.43	230
Eye	0.51	198
Muscles	0.11	900
Blood	1.0	100
CSF	1.82	55
Other neural tissue	0.16	624
Internal air	0.002	50000 [24]

where σ is the electrical conductivity tensor, Φ is the electrical potential, $\mathbf{J}^i$ is the current source density, $\mathbf{n}$ is a vector normal to the surface, Ω is the volume of the head, and Γ_Ω is the surface of the head [19].

B. The Half Sensitivity Volume

In [20] the concept of half-sensitivity volume (HSV) was applied to define the volume of the source region in which the sensitivity of the measurement lead is concentrated. The HSV is the size of the volume within the source region of the volume conductor, where the magnitude of the detector's sensitivity is at least half of its maximum density. The smaller the HSV is, the smaller the region from which the majority of the detector's signal arises. The half-sensitivity volume is thus applied to compare the detector's ability to concentrate its measurement sensitivity. In this study, the source region is defined as the gray matter, which is the area where neuroelectric activity is generated. However, we also compute the HSV from the gray and white matter combined, which measures the total brain region.

C. Model and computations

We calculate the sensitivity distributions in a realistically shaped male head model based on the Visible Human Project man dataset [21]. The tissues and their corresponding conductivities (resistivities) are listed in Table I [22]. Calculations of the sensitivity distributions are based on the principle of reciprocity and the solution of the numerical finite difference method (FDM) of the EEG electrode sensitivity. In the present study we apply the scalp-to-skull conductivity ratio of 15:1 [23]. We calculate the sensitivity distributions of the brain for twenty-four bipolar electrode pairs located subdermally on the exterior surface of the skull. The size of each subdermal electrode measures 1 mm $\times$ 1 mm $\times$ 1 mm, which reflects the size of one voxel. Our bipolar leads detect frontal cortex activity, where the reference is located slightly sinister to the 10/20 location C_Z. The twenty-five electrodes are spaced 5 mm apart both laterally and anterior-posteriorly in a five-by-five grid such that the center electrode is the reference at C_Z.

TABLE II
HSV RESULTS OF THE GRAY MATTER OF THE VISIBLE HUMAN MAN (VHM) BIPOLAR LEAD PAIRS. THE RESULTS PROGRESS FROM ANTERIOR TO POSTERIOR BY READING THE TABLE FROM TOP TO BOTTOM WITH SPACING OF 5 MM PER ROW. THE COLUMNS ARE SPACED 5 MM APART FROM SINISTER TO DEXTER ELECTRODE LOCATIONS.

Location	Sinister -10 mm $[mm^3]$	Sinister -5 mm $[mm^3]$	Center 0 mm $[mm^3]$	Dexter 5 mm $[mm^3]$	Dexter 10 mm $[mm^3]$
Anterior 10 mm	73	38	32	96	226
Anterior 5 mm	53	28	24	96	137
Center 0 mm	52	28	ref	73	100
Posterior 5 mm	103	88	189	172	84
Posterior 10 mm	188	189	266	161	116

TABLE III
HSV RESULTS OF THE GRAY MATTER AND WHITE MATTER COMBINED, I.E. WHOLE BRAIN, OF THE VISIBLE HUMAN MAN (VHM) BIPOLAR LEAD PAIRS. THE RESULTS PROGRESS FROM ANTERIOR TO POSTERIOR BY READING THE TABLE FROM TOP TO BOTTOM WITH SPACING OF 5 MM PER ROW. THE COLUMNS ARE SPACED 5 MM APART FROM SINISTER TO DEXTER ELECTRODE LOCATIONS.

Location	Sinister -10 mm $[mm^3]$	Sinister -5 mm $[mm^3]$	Center 0 mm $[mm^3]$	Dexter 5 mm $[mm^3]$	Dexter 10 mm $[mm^3]$
Anterior 10 mm	151	63	51	140	328
Anterior 5 mm	93	36	34	122	163
Center 0 mm	78	39	ref	99	106
Posterior 5 mm	145	119	255	224	93
Posterior 10 mm	304	258	405	231	168

III. RESULTS

Tables II and III show that the implantation of the subdermal electrode focuses and concentrates the HSV within the gray matter and to the whole brain, respectively. The gray matter HSVs (Table II) of these source regions indicate an increase in the volume from 33% to 86% from which the neuroelectric activity is measured when the electrodes increase their spacing from 5 mm to 10 mm from the reference electrode. Three of the four diagonal measurements increased in HSV from 114% to 161% with the most dexter posterior corner decreasing in HSV by 33%. Furthermore, there are a few electrodes in the most posterior row and dexter corner that do not increase in HSV because the respective lead fields are not parallel to each other.

Fig. 1 and Fig. 2 illustrate the subdermal measurement sensitivity distributions on the cortex and in sagittal and coronal cross sections of the gray matter. The distributions clearly concentrate the measurement sensitivity to the target region between the minimally-invasive measurement pairs and eliminate much of the scalp and skull smearing from the traditional surface measurements. Precisely, the subdermal leads measure neuroelectric activity on or near the gyral cortical surface rather than sulcal or deep sources (Fig. 1e & f). Moreover, the measurement sensitivity distributions clearly increase in extent when comparing the 10 mm to the 5 mm subfigures. Fig. 2 illustrates that the grid of subdermal electrodes is slightly displaced towards the sinister side of the body.

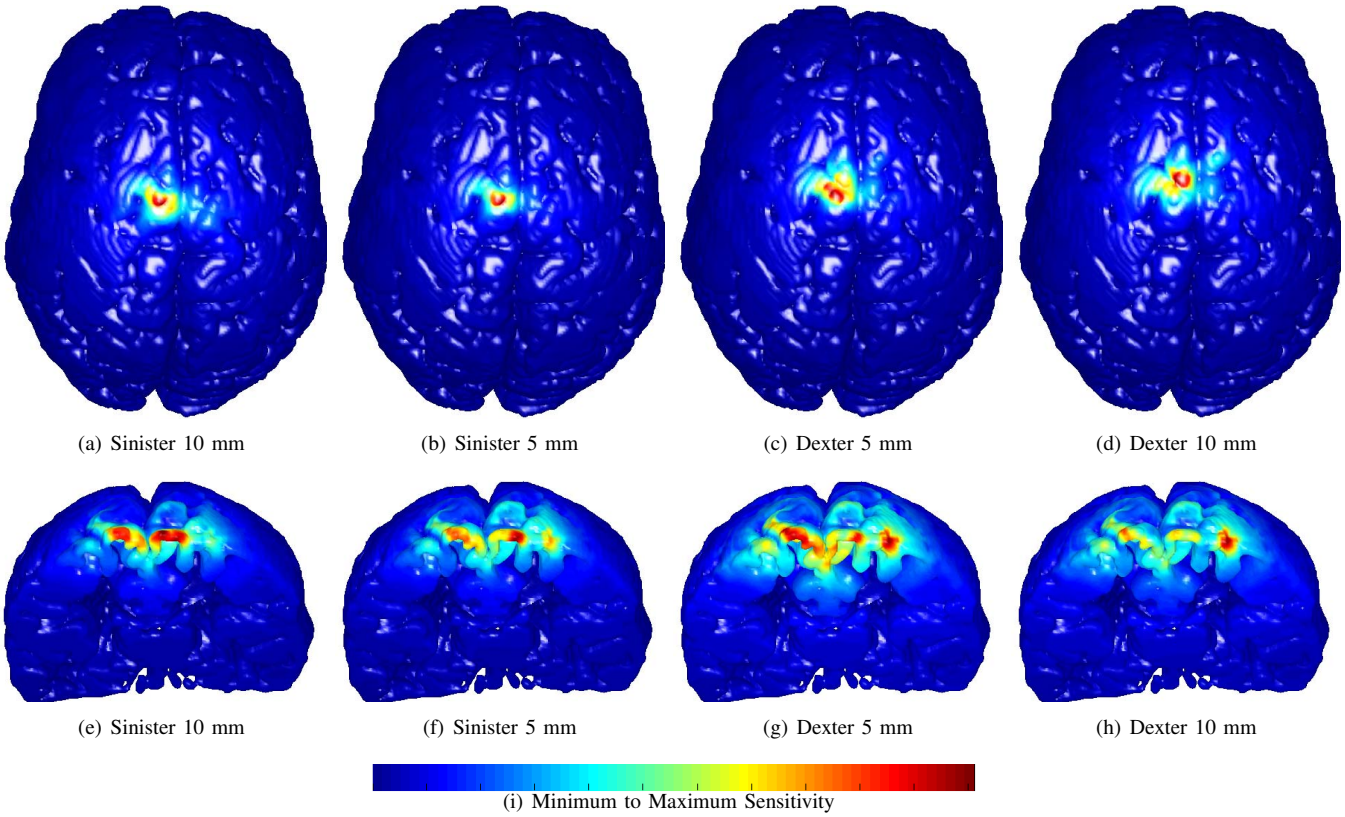

(a) Sinister 10 mm (b) Sinister 5 mm (c) Dexter 5 mm (d) Dexter 10 mm

(e) Sinister 10 mm (f) Sinister 5 mm (g) Dexter 5 mm (h) Dexter 10 mm

(i) Minimum to Maximum Sensitivity

Fig. 1. The lateral spacing of the source to sink measurement electrodes is 5 mm and 10 mm. The reference electrode is the same electrode for each pair located along the central sulcus near C_Z. (a – d) Cortical sensitivity distributions. (e – h) Gray matter coronal cross section.

IV. Discussion

We analyzed our realistic models to identify the phenomenon of EEG measurement sensitivity distributions. We found that the HSV decreases in volume as the electrodes move closer together for subdermal electrodes just like the traditional surface electrodes [16], [20]. This decrease means that the sensitivity is more concentrated in the gray matter, optimally detecting sources parallel to the lead field. The optimal detection of the parallel sources would come from radial sources in the gyrus underneath and slightly shifted in the direction of the reference electrode and from tangential sources in the walls of the gray matter leading into the sulci between the bipolar lead pair [25]. The density and direction of the lead field current indicates the measurement sensitivity distributions in a volume conductor [26]–[28]. The colorbars (Figs. 1 & 2i) demarcate the density of the lead field, whereas the direction would be the lead field current flowlines between the electrodes.

Our numerical results indicate that the subdermal leads measure rather focused volumes (Figs. 1 & 2). These concentrated measurement leads improve the signal-to-noise ratio (SNR) and reduce the number of epochs because each lead detects less background activity, thus requiring less signal averaging [29]. Although these minimally-invasive subdermal electrodes benefit the patient and the recording session, the sensitivity distributions vary in size even when comparing equidistant electrode pairs with respect to a common reference electrode (Tables II & III).

We believe when the electrodes are as near as 5 mm and 10 mm, this effect is due to varying gray matter thickness over the cortex, varying sizes of gyri and sulci, and varying volumes of the CSF filling the respective sulci. Furthermore, we believe that the variation can be additionally due to placement of bipolar subdermal electrodes across a sulci i.e. between different gyri. This is evident in our dexter-posterior results (Tables II & III) as we have purposely slightly shifted the electrode grid sinister from the midsagittal line in order not to directly place subdermal electrodes over a sulcus. Moreover, we verified that the CSF was not continuous in this VHM model, which left patches of gray matter exposed directly to the skull. There was a direct correlation with missing or very thin CSF directly under an electrode to a low HSV, i.e. a very focused measurement (Tables II & III). This is opposed to very thick CSF pooling in a sulcal cavity directly underneath an electrode that yields a very high HSV that diffuses the lead field currents [30]. This study should be applied to another model that has continuous CSF coverage protecting the gray matter from the skull.

The skull thickness is rather smooth in the cranial vault so this thickness would minimally influence the variance of the HSVs across a lobe. Such bones as the frontal, parietal and temporal bones gradually vary in thickness and geome-

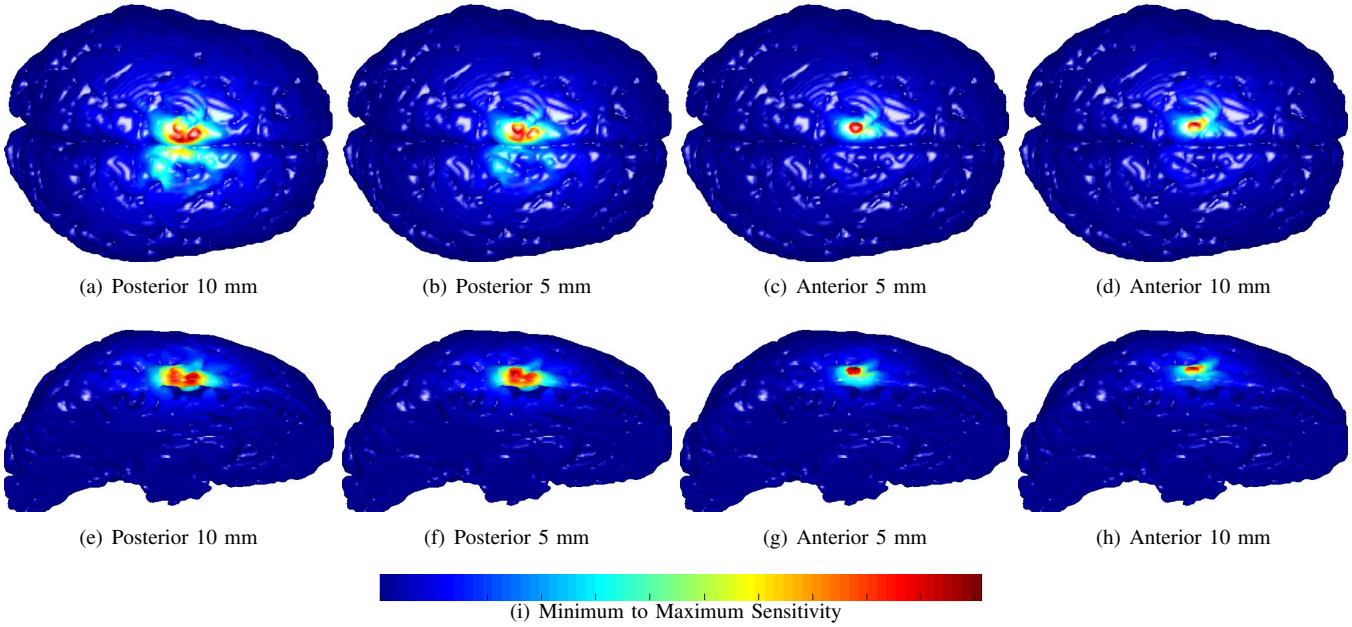

(a) Posterior 10 mm (b) Posterior 5 mm (c) Anterior 5 mm (d) Anterior 10 mm

(e) Posterior 10 mm (f) Posterior 5 mm (g) Anterior 5 mm (h) Anterior 10 mm

(i) Minimum to Maximum Sensitivity

Fig. 2. Anterior to posterior spacing of source to sink measurement electrodes is 5 mm and 10 mm. The reference electrode is the same electrode for each pair located slightly sinister to the central sulcus near C_Z. (a – d) Cortical sensitivity distributions. (e – h) Gray matter saggital cross section.

try except near the sutures. Therefore, the general behavior of the subdermal lead's measurement sensitivity distribution increases with increasing distance and measures relatively similarly when comparing to measurements at different depths [1]. However, the ability to locate subdermal electrodes even more closely to each other than traditional high resolution EEG montages causes much variance in measurement sensitivity volumes, specifically HSVs. We surmise that this could benefit source localization and source imaging techniques as the varying CSF, gyri, and gray matter thickness would behave as a weighting for each lead pair. Additionally, these techniques would benefit due to the bypassed skin because of the subdermal placement of the lead.

V. Conclusion

The usage of small subdermal electrodes significantly reduces the minimum distance required between traditional surface EEG electrodes. This benefit allows the clinician to probe around very specifically for foci such as an epileptic focus or a known evoked potential. These concentrated minimally-invasive measurements will allow clinicians and researchers to obtain more information of the underlying neuroelectric processes without the need for the highly invasive cortical electrodes. Although these subdermal leads record with improved SNRs, continued investigations should determine the optimal bipolar separation to measure only one gyrus at a time. This precursory study indicates most bipolar subdermal pairs spaced equal to or closer than 10 mm will measure cortical activity from a single gyrus. The future studies will further determine the actual location of the sources.

Acknowledgment

The authors would like to thank Noriyuki Takano PhD for providing the finite difference method software and Gunnar Seemann for providing the segmented Visible Human Man. The authors would also like to thank the Department of Biomedical Engineering and the International Graduate School in Biomedical Engineering and Medical Physics, Finland, for funding this research.

References

[1] J. Väisänen, K. Wendel, G. Seemann, J. Malmivuo, and J. Hyttinen, "Sensitivites of bipolar subcutaneous and cortical eeg leads," in *IFMBE Proceedings*, O. Dössel and W. Schlegel, Eds., vol. 25. Munich, Germany: World Congress 2009, 2009, pp. 267–270.

[2] K. Wendel, J. Väisänen, G. Seemann, J. Hyttinen, and J. Malmivuo, "The influence of age and skull conductivity on surface and subdermal bipolar EEG leads," *Computational Intelligence and Neuroscience*, vol. 2010, no. 397272, p. 7 pages, 2010.

[3] L. Zablow and E. Goldensohn, "A comparison between scalp and needle electrodes for the EEG," *Electroencph. Clin. Neurophysiol.*, vol. 26, pp. 530–533, 1969.

[4] J. Siivola and M. Järvilehto, "Spinal evoked potentials evaluated with two relevant electrode types," *Acta Physiol Scan*, vol. 115, no. 1, pp. 103–107, 1982.

[5] D. Dumitru and J. Lester, "Needle and surface electrode somatosensory evoked potential normative data: a comparison," *Arch Phys Med Rehabil*, vol. 72, no. 12, pp. 989–992, November 1991.

[6] T. Hemmerling, C. Coimbra, P. Harvey, and M. Choinière, "Needle electrodes can be used for bispectral index monitoring of sedation in burn patients," *Anesthesia Analgesia*, vol. 95, pp. 1675–1677, 2002.

[7] G. Young, J. Ives, M. Chapman, and S. Mirsattari, "A comparison of subdermal wire electrodes with collodion-applied disk electrodes in long-term EEG recordings in ICU," *Clin. Neurophysiol.*, vol. 117, pp. 1376–1379, 2006.

[8] G. Martz, C. Hucek, and M. Quigg, "Sixty day continuous use of subdermal wire electrodes for EEG monitoring during treatment of status epilepticus," *Neurocrit Care*, vol. 11, pp. 223–227, May 2009.

[9] T. Hemmerling and P. Harvey, "Electrocardiographic electrodes provide the same results as expensive special sensors in the routine monitoring of anesthetic depth," *Anesth Analg*, vol. 94, pp. 369–371, 2002.

[10] P. Akavipat, K. Dumrongbul, and P. Neamnak, "Can electrocardiogram electrodes replace bispectral index electrodes for monitoring depth of anesthesia?" *J Med Assoc Thai*, vol. 89, no. 1, pp. 51–55, 2006.

[11] P. Sebel, T. Bowdle, M. Ghoneim, I. Rampil, R. Padilla, T. Gan, and K. Domino, "The incidence of awareness during anesthesia: a multicenter United States study," *Anesth Analg*, vol. 99, pp. 833–839, 2004.

[12] T. McCulloch, "Use of BIS Monitoring Was Not Associated with a Reduced Incidence of Awareness," *Anesth Analg*, vol. 100, no. 4, p. 1221, 2005.

[13] V. Jäntti and S. Alahuhta, "The BIS inverse problem and pharmacodynamics," *Anesthesiology*, vol. 97, no. 3, pp. 756–757, September 2002.

[14] D. Dumitru, G. Powell, and J. King, "The effect of different needle recording electrodes on somatosensory-evoked potentials and intertrial waveform variation," *Am J Phys Med Rehabil*, vol. 71, no. 3, pp. 164–169, June 1992.

[15] R. Plonsey, "Reciprocity applied to volume conductors and the EEG," *IEEE Trans Biomed Electron*, vol. 10, no. 1, pp. 9–12, 1963.

[16] J. Malmivuo and R. Plonsey, *Bioelectromagnetism — Principles and Applications of Bioelectric and Biomagnetic Fields*. New York: Oxford University Press, 1995.

[17] H. Helmholtz, "Über einige Gesetze der Vertheilung elektrischer Ströme in körperlichen Leitern mit Anwendung auf die thierischelektrischen Versuche." *Ann Phys Chem*, vol. 89, pp. 211–233, 354–377, 1853.

[18] J. Sarvas, "Basic mathematical and electromagnetic concepts of the biomagnetic inverse problem," *Phys. Med. Biol.*, vol. 32, no. 1, pp. 11–22, 1987.

[19] C. Johnson, M. Mohr, U. Rude, A. Samsonov, and K. Zyp, *Multiscale and Multiresolution Methods in Computational Science and Engineering*. Berlin: Springer, 2003, ch. Multilevel methods for inverse bioelectric field problems.

[20] J. Malmivuo, V. Suihko, and H. Eskola, "Sensitivity distributions of EEG and MEG measurements," *IEEE Trans Biomed Eng*, vol. 44, no. 3, pp. 196–208, March 1997.

[21] F. Sachse, C. Werner, K. Meyer-Waarden, and O. Dössel, "Applications of the visible man dataset in electrocardiology: Calculation and visualization of body surface potential maps of a complete heart cycle," in *Proc. of the Second Users Conference of the National Library of Medicine's Visible Human Project*, 1998, pp. 47–48.

[22] C. Ramon, P. Schimpf, and J. Haueisen, "Influence of head models on EEG simulations and inverse source localizations," *BioMedical Engineering Online*, 5:10 2006.

[23] T. Oostendorp, J. Delbeke, and D. Stegeman, "The conductivity of the human skull: Results of in vivo and in vitro measurements," *IEEE Trans Biomed Eng*, vol. 47, no. 11, pp. 1487–1492, November 2000.

[24] J. Haueisen, C. Ramon, M. Eiselt, H. Brauer, and H. Nowak, "Influence of tissue resistivities on neuromagnetic fields and electric potentials studied with a finite element model of the head," *IEEE Trans Biomed Eng*, vol. 44, no. 8, pp. 727–735, August 1997.

[25] K. Wendel, O. Väisänen, J. Malmivuo, N. Gencer, B. Vanrumste, P. Durka, R. Magjarević, S. Supek, M. Pascu, H. Fontenelle, and R. Grave de Peralta Menendez, "EEG/MEG source imaging: Methods, challenges, and open issues," *Computational Intelligence and Neuroscience*, vol. 2009, no. 656092, p. 12 pages, 2009.

[26] R. McFee and F. Johnston, "Electrocardiographic leads I. Introduction," *Circulation*, vol. 8, no. 10, pp. 554–568, 1953.

[27] ——, "Electrocardiographic leads II. Analysis," *Circulation*, vol. 9, no. 2, pp. 255–266, 1954.

[28] ——, "Electrocardiographic leads III. Synthesis," *Circulation*, vol. 9, no. 6, pp. 868–880, 1954.

[29] A. Joutsen, L. Lyytikäinen, J. V. J. Jurva, K. Wendel, O. Väisänen, J. Tanskanen, V. Jäntti, and H. Eskola, "Median nerve somatosensory evoked potential recordings using surface and needle electrodes," in *Proceedings of the* 29^{th} *Intl. Congress of Clinical Neurophysiology*, vol. Oct 28 – Nov 2. ICCN, 2010, pp. Kobe, Japan.

[30] K. Wendel, N. Narra, M. Hannula, P. Kauppinen, and J. Malmivuo, "The Influence of CSF on EEG Sensitivity Distributions of Multilayered Head Models," *IEEE Trans Biomed Eng*, vol. 55, no. 4, pp. 1454–1456, April 2008.